

# A comprehensive model using modified Zeeman model for generating ECG signals

A Ayatollahi, N Jafarnia Dabanloo, DC McLernon, V Johari Majd, H Zhang

**Abstract:** Developing a mathematical model for the artificial generation of electrocardiogram (ECG) signals is a subject that has been widely investigated. One of its uses is for the assessment of diagnostic ECG signal processing devices. So the model should have the capability of producing a wide range of ECG signals, with all the nuances that reflect the sickness to which humans are prone, and this would necessarily include variations in heart rate variability (HRV). In this paper we present a comprehensive model for generating such artificial ECG signals. We incorporate into our model the effects of respiratory sinus arrhythmia, Mayer waves and the important very low frequency component in the power spectrum of HRV. We use the new modified Zeeman model for generating the time series for HRV, and a single cycle of ECG is produced using a radial basis function neural network.

**Keywords:** ECG, neural networks, heart rate variability, dynamical systems.

## 1 Introduction

The electrocardiogram (ECG) signal is one of the most obvious effects of the human heart operation. The oscillation between systole and diastole states of the heart is reflected in the heart rate (HR). The surface ECG is the recorded potential difference between two electrodes placed on the surface of the skin in predefined points. The largest amplitude of a single cycle of the normal ECG is referred to as the R-wave. The time between successive R-waves is referred to as an RR-interval, and an RR tachogram is then a series of RR-intervals. Variability in this time series has been widely used as a measure of heart operation, and it reveals important information about the physiological state of the subject [1]. Analysis of variations in this time series is known as heart rate variability (HRV) analysis [2], and the development of a dynamical model for the artificial generation of electrocardiogram (ECG) signals is a subject that has been widely investigated. One of its uses is for the assessment of diagnostic ECG signal processing devices.

In constructing a comprehensive model for generating ECG signals there are two steps. Step one is producing the artificial RR tachogram, and step two is constructing the actual shape of the ECG. The RR tachogram shows where the R-waves of the ECG are actually placed.

The dynamic response of the cardiovascular control system to physiological changes is reflected in HRV and blood pressure. Recent attention has focused on what HRV signifies in term of cardiovascular health, and HRV is being investigated as a high-risk indicator for possible mortality following myocardial infraction [3]. Beat-to-beat variations of human RR-intervals display fluctuations over a number of different time scales

ranging from seconds to days. Some of these fluctuations are relatively well understood and arise from: (i) the interactions between different physiological control mechanisms such as respiratory sinus arrhythmia (RSA) and Mayer waves; (ii) the amount of physical and mental activity; (iii) the circadian rhythm; and (iv) the effects of different sleep stages [4]. Producing a time series for HRV is an important aspect in generating an artificial ECG signal.

The motivation for using nonlinear methods in modeling HRV is that the source of the mechanism (i.e. the electrical properties of myocardial fiber) is nonlinear. In 1972, Zeeman presented a nonlinear dynamical structure for heartbeat modeling [5], based on the Van der Pol-Lienard equation, but this model did not entirely satisfy the biologists understanding of HRV generation [6]. The reason was the lack of consideration given to important biological parameters such as sympathetic and parasympathetic activities. Here, we will use a new modified Zeeman model to produce the RR tachogram signal. We will try to incorporate the effects of sympathetic and parasympathetic activities so that we generate the significant peaks in the power spectrum of HRV. For the actual shape of the ECG in a single cycle we use a neural network approach based upon a modified McSharry model.

This paper is organized as follows. In section 2, a summary of ECG and HRV morphology is given. The proposed model is developed in section 3. Simulation results will be given in section 4, and finally conclusions are presented in section 5.

## 2 ECG and HRV morphology

In any heart operation there are a number of important events. The successive atrial depolarization/repolarization and ventricular depolarization/repolarization occurs with every heartbeat. These are associated with the peaks and valleys of the ECG signal, which are traditionally labeled P,Q,R,S, and T (see Fig.1). The P-wave is caused by depolarization of the atrium prior to atrial contraction. The QRS-complex is caused by ventricular depolarization prior to ventricular contraction. The largest amplitude signal (i.e. R-wave) is located here. The T-wave is caused by ventricular repolarization which lets the heart be prepared for the next cycle. Atrial repolarization occurs before ventricular

---

Iranian Journal of Electrical & Electronic Engineering, 2005.

Paper first received 8th November 2004 and in revised from 10th July 2005.

A Ayatollahi and N Jafarnia Dabanloo are with the Department of Electrical Engineering Iran University of Science and Technology, Narmak, Tehran 16844, Iran. DC McLernon is with School of Electronic and Electrical Engineering in the University of Leeds, Leeds, UK. V Johari Majd is with Electrical Engineering Department Tarbiat Modares University, Tehran, Iran and H Zhang is with Biology Department Leeds University, Leeds, UK.

depolarization, but its waveform is masked by the large amplitude QRS-complex.

The heart rate, which is the inverse of the RR-interval, directly affects the blood pressure. The Autonomic Nervous System (ANS) is responsible for short-term regulation of the blood pressure. The ANS is a part of the Central Nervous System (CNS). The ANS uses two subsystems - the sympathetic and parasympathetic systems. The heart rate may be increased by slow acting sympathetic activity or decreased by fast acting parasympathetic (vagal) activity. The balance between the effects of the sympathetic and parasympathetic systems is referred to as the sympathovagal balance and is believed to be reflected in the beat-to-beat changes of the cardiac cycle [4]

Spectral analysis of HRV is a useful method to investigate the effects of sympathetic and parasympathetic activities on heart rate (HR). The afferent nerves provide the feedback information to the CNS. The slow acting sympathetic activity can increase the HR up to 180 beats per minute (bpm). The sympathetic system is active during stressful conditions. When sympathetic activity increases after a latent period of up to 5 seconds, a linearly dependent increment in HR begins and reaches its steady state after about 30 seconds. This affects the low frequency (LF) component (0.04-0.15 Hz) in the power spectrum of the HRV, and slightly alters the high frequency (HF) component (0.15-0.4 Hz) (RSA component). The fast acting parasympathetic activity can decrease the HR down to 60 bpm. The parasympathetic system is active during rest conditions. There is a linear relation between decreasing the HR and the parasympathetic activity level, without any considerable latency. This affects only the HF in the power spectrum of the HRV. The power in the HF section of the power spectrum can be considered as a measure for parasympathetic activity. The power ratio LF/HF can be considered as a measure of the balance between the effects of sympathetic and parasympathetic systems [1]. Fig 2 shows a typical power spectrum of a healthy person.

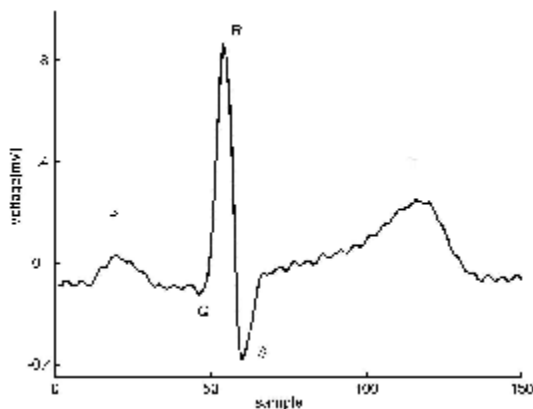


Fig. 1 A single cycle of an ECG signal.

Our model will produce a typical power spectrum as shown in Fig. 2. But for different sicknesses the model has the capability to alter both the magnitudes, and central frequencies, of the peaks of the power spectrum to reflect different illnesses.

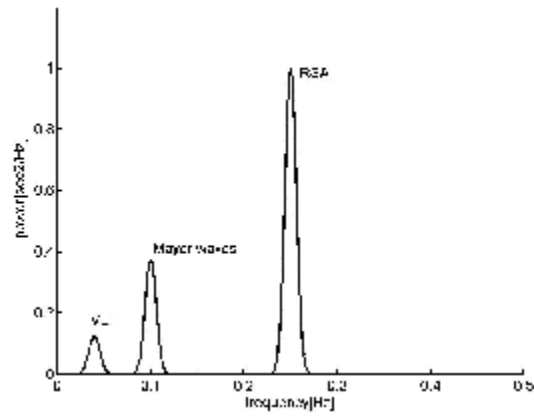


Fig. 2 A typical power spectrum of HRV for a healthy patient.

### 3 Our proposed model for ECG generation

Let start with the first step. As regards ECG generation, Zeeman [5] introduced a nonlinear dynamic system of three inter-coupled differential equations as follows:

$$\begin{aligned} \varepsilon \dot{x} &= -(x^3 + ax + b) \\ \dot{a} &= -2x - 2a \\ \dot{b} &= -a - 1 \end{aligned} \quad (1)$$

where  $x$  (which can be negative) is related to the length of the heart muscle fiber,  $\varepsilon$  is a positive scalar,  $b$  is a parameter representing an electrochemical control,  $x_0$  is the initial length of the heart muscle in the diastole state, and parameter  $a$  is related to the tension in the muscle fiber. We can get the equilibrium point of this dynamical system by solving the following equations:

$$\begin{aligned} -(x^3 + ax + b) &= 0 \\ -2x - 2a &= 0 \\ -a - 1 &= 0. \end{aligned} \quad (2)$$

So there is an equilibrium point at  $A(1, -1, 0)$ . Now we want to find a linear approximation of the system in the neighborhood of  $A$ , and so we can write [5]:

$$\begin{bmatrix} \dot{x} \\ \dot{a} \\ \dot{b} \end{bmatrix} = \begin{bmatrix} -2 & -1 & -1 \\ \varepsilon & \varepsilon & \varepsilon \\ 0 & -1 & 0 \end{bmatrix} \begin{bmatrix} x \\ a \\ b \end{bmatrix}. \quad (3)$$

The square matrix in (3) has eigenvalues  $(-1 \pm i\sqrt{3})/2$  and  $(-2)/\varepsilon$ . Thus the point  $A(1, -1, 0)$  is a stable equilibrium point. Now, because  $\varepsilon$  is very small the 'fast' eigenvalue (with direction parallel to  $x$ -axis) is  $(-2)/\varepsilon$ . As  $|(-1 \pm i\sqrt{3})/2|$  is small (compared to  $(-2)/\varepsilon$ ), the two complex eigenvalues indicate a steady slow direction toward  $A$ . Fig 3 shows the trajectory of the above model in phase-space (parameterized by time). Now we can consider the variation of  $-x$  vs. time (see Fig. 4) as a potential action which repeats in time as heart beating, because it has a stable oscillation with different behavior in its path (like an action potential). Note the rapid jumps from  $B$  to  $C$  (like from diastole to systole state) and the slow return from  $C$  to  $A$  (like from systole to diastole state), as shown in Fig. 4.

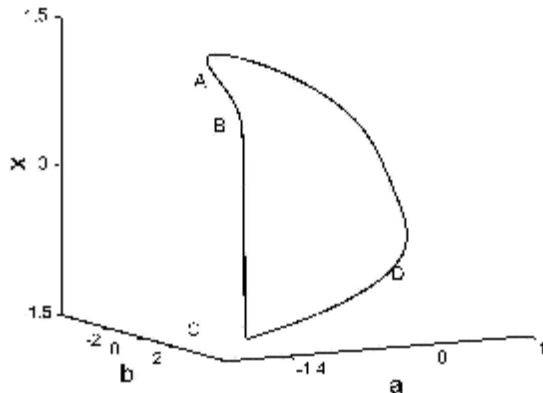


Fig. 3 Trajectory of heart model states in (1).

In order to control the repeat cycle of the trajectory in (1), we add an additional control parameter (i.e.  $\delta$ ) and get the following system:

$$\begin{aligned} \varepsilon \dot{x} &= -(x^3 + ax + b) \\ \delta \dot{a} &= -2x - 2a \\ \delta \dot{b} &= -a - 1. \end{aligned} \quad (4)$$

It is easy to see that the frequency of the oscillation in this model depends on the values of  $\delta$ . This relation is more or less linear - see Fig. 5.

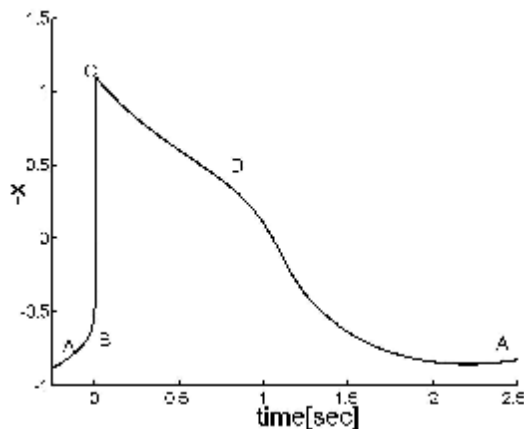


Fig. 4 Action potential produced by (1).

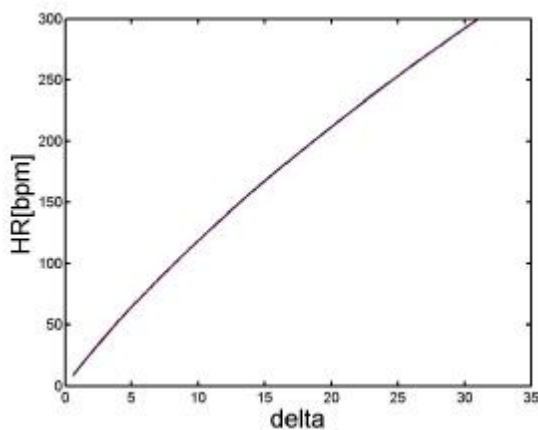


Fig. 5 Graph HR vs.  $\delta$ .

Now if we relate the parameter  $\delta$  to the four virtual states (i.e.  $s_1$ ,  $s_2$ ,  $p_1$ , and  $p_2$  corresponding to sympathetic and parasympathetic activity levels), we can change the value of  $\delta$  with proper sinusoidal variations according to our hypothesis for sinusoidal variations of sympathetic and parasympathetic activities. The eqns in (5) simply show the sinusoidal variations for these four virtual states:

$$\begin{aligned} \ddot{s}_1 &= -\omega_1^2 s_1 \\ \ddot{s}_2 &= -\omega_2^2 s_2 \\ \ddot{p}_1 &= -\omega_3^2 p_1 \\ \ddot{p}_2 &= -\omega_4^2 p_2 \end{aligned} \quad (5)$$

and we can relate these values to the parameter  $\delta$  by the following equations:

$$\begin{aligned} q_1 &= c_1 (s_1 + 1) + c_2 (s_2 + 1) \\ q_2 &= c_3 (p_1 + 1) + c_4 (p_2 + 1) \\ q &= q_1 - q_2 \\ \delta &= h(q). \end{aligned} \quad (6)$$

The parameter  $\delta$  determines the HR, and the function  $h$  and the coupling factors ( $c_1$ ,  $c_2$ ,  $c_3$ , and  $c_4$ ) determine how the sympathetic and parasympathetic activities alter the HR. Finally, the parameters  $\omega_1$ ,  $\omega_2$ ,  $\omega_3$ , and  $\omega_4$  are the angular frequencies for the sinusoidal variations of the sympathetic and parasympathetic activities. In order to choose the values of  $\omega_1$ ,  $\omega_2$ ,  $\omega_3$ , and  $\omega_4$ , we provide the following hypotheses [1-4]:

- i) The most important contribution to changes in HRV is the effect of RSA, which is believed to be produced by fluctuations of vagal-cardiac nerve activity. It produces the HF component of the HRV power spectrum. The HR accelerates during inspiration and decelerates during expiration, and the magnitude of this response depends on the rate and depth of respiration. Because of the latent response of the sympathetic system and its low-pass filtering behavior, we consider the respiration response only in the parasympathetic system. So  $\omega_4$  will be related to the frequency of respiration.
- ii) The LF component which occurs around 0.1 Hz, originates from self-oscillation in the vasomotor part of the baroreflex loop as a result of negative feedback in the baroreflex. This fluctuation is synchronous with fluctuations of blood pressure, and it is known as the Mayer wave. This fluctuation decreases with both parasympathetic and sympathetic blockade. So  $f_2$  and  $f_3$  are related to 0.1 Hz, where  $\omega_i = 2\pi f_i$ .
- iii) The very low frequency (VLF) component, which is believed to arise from thermoregulatory peripheral blood flow adjustments, is caused by the sympathetic nervous system. So  $\omega_1$  is related to this frequency.

- iv) We assume that there is no inter-coupling between sympathetic and parasympathetic activities.

But although this function  $h(q)$  (in (6)) is nonlinear, it can be approximated with either piecewise linear modules (as we will do in this paper) or with a neural network (currently research in progress by the authors).

Now, the timing of  $(-x)$  gives us the RR-intervals – see Fig. 4. This is an approximation to the time series of RR time intervals (i.e.  $T_{RR}(t)$ ), and let us call it  $\hat{T}_{RR}(t)$ . We will then have:

$$\omega(t) = \frac{2\pi}{\hat{T}_{RR}(t)}. \quad (7)$$

We are ready to use the time series generated by the modified Zeeman model in another dynamical system which will produce the shape of the ECG signal in a single cycle and both together generate the complete ECG.

Consider the system of three inter-coupled differential equations in  $x_1, x_2, x_3$  and  $t$  (see (8)). It always results in a stable limit cycle, whose projection onto the  $x_1$ - $x_2$  plane is a circle. But the projection onto the  $x_3$ -axis, when plotted against time, can be shown to give the required artificial ECG signal,  $\hat{f}(t)$  - where  $f(t)$  is the original ECG signal over one cycle – see Fig. 6.

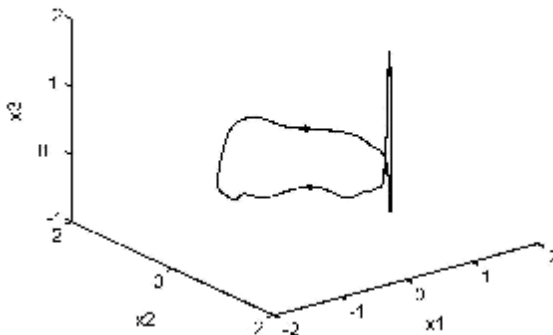


**Fig. 6** A typical limit cycle in time-parameterized  $x_1$ - $x_2$ - $x_3$  space.

We have modified the dynamic equations from [1] to get:

$$\begin{aligned} \dot{x}_1 &= \omega(t)x_2 + x_1(1 - x_1^2 - x_2^2) \\ \dot{x}_2 &= -\omega(t)x_1 + x_2(1 - x_1^2 - x_2^2) \\ \dot{x}_3 &= \hat{g}(\theta) - x_3. \end{aligned} \quad (8)$$

Now, in (8)  $\omega(t)$  corresponds to the angular velocity of the limit cycle in the  $x_1$ - $x_2$  plane, and we have:

$$\theta = \text{angle}(x_1 + jx_2) / 2\pi, 0 \leq \theta < 1$$

We consider a single cycle of a normal or abnormal real ECG signal ( $f(t)$ ) with a (normalized) period of one second. Note that  $t$  and  $\theta$  are interchangeable over one cycle of  $f(t)$  (the original ECG). If:

$$g(t) \cong Tdf(t)/dt$$

then we generate the approximation of  $g(t)$  with the following expansion:

$$\hat{g}(\theta) = \sum_{i=1}^N w_i \exp(-(\theta - t_i)^2 / (2\sigma_i^2)). \quad (9)$$

Suppose we take  $m$  samples of  $f(t)$ . We then use a low-pass digital filter to attenuate any noise. The next step is to calculate the scaled derivative of  $f(t)$ , by using the backward difference approximation,  $g(t)$ :

$$\begin{aligned} \mathbf{f} &= [f(0), f(T), \dots, f((m-1)T)], \\ g(jT) &= f(jT) - f((j-1)T). \end{aligned} \quad (10)$$

The centers  $\{t_i\}$  in (9) can be assigned directly based on our ECG knowledge, or with an unsupervised algorithm, we have decided here to estimate all the parameters  $\{\omega_i, t_i, \sigma_i\}$  with a gradient-descent procedure - for more details refer to [7].

As is already known, the RBF neural network has fast adaptation, and because of its nonlinear kernels it can easily approximate our proposed nonlinear dynamic. The ability of an RBF neural network to approximate any nonlinear function has been proven by Park and Sandberg [8]. But it is slower than the backpropagation approach in the recall phase.

#### 4 Simulation results

In the off-line phase of the simulation, the RBF neural network (with one hidden layer) produces the approximation of  $g(t)$ . At first, we filter the derivative ( $g(t)$ ) of the desired ECG signal ( $f(t)$ ), in order to reduce the required number of neurons. We then feed the data into the learning process of the RBF neural network, and obtain the required parameters  $\{\omega_i, t_i, \sigma_i\}$  - i.e. weights, centers and spread factors. So from this method we can obtain the parameters for the normal ECG, ECG with Wolf-Parkinson-White (WPW), ECG with hyper kalmia and finally ECG with ventricular flutter.

Then in the online phase, we start a discrete-time simulation of the model in (8), with an arbitrary initial values for  $x_1, x_2$ , and  $x_3$  with the generated RR-intervals. Of course for the four different ECG signals, we simply supply the model in (7) with the required parameters and the model generates the artificial ECG.

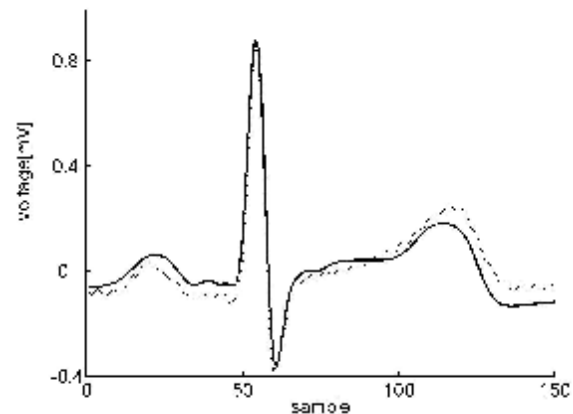


**Fig. 7** A single cycle of a simulated normal ECG (dotted for the original).

One cycle of the simulated normal ECG and the original ECG is shown in Fig. 7, for comparison purposes. The error measure, which determines how closely we actually simulate the required ECG ( $f(t)$ ), is the Total Error Per Cycle (TEPC) in (11), where  $\hat{f}$  is the actual output of the model.

$$TEPC = \frac{100}{\max(|f|)} \sqrt{\frac{\sum_{j=0}^{m-1} (f(jT) - \hat{f}(\theta_j))^2}{m}} \quad (11)$$

The result of plotting  $TEPC$  in (11) versus different numbers ( $N$ ) of neurons is shown in Table 1 for the four different ECG's associated with normal ECG, WPW syndrome, hyper-kalmia, and ventricular flutter.

**Table 1**  $TEPC$  errors (based on (10)) for the four simulated ECG signals.

N	TEPC1	TEPC2	TEPC3	TEPC4
5	15.4809	11.6789	25.0097	5.6707
10	6.8249	10.1976	8.2338	2.6610
15	3.2790	5.3811	2.8298	1.0802
20	2.3551	3.8720	1.1634	0.9260

The results for the  $TEPC1$  vs.  $N$  for the normal ECG in Table 1, are given in more detail in Fig.8. In addition, the simulated abnormal ECG signals are shown in Figs 9, 10 and 11, corresponding respectively to WPW syndrome, hyper-kalmia and ventricular flutter.

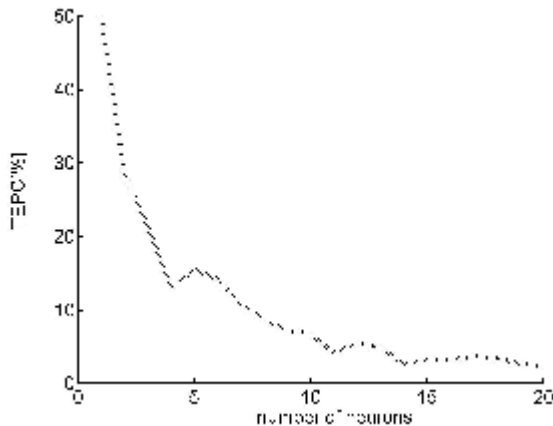


**Fig. 8**  $TEPC$  measure (see (11)) for the simulated normal ECG v.s. number of neurons.

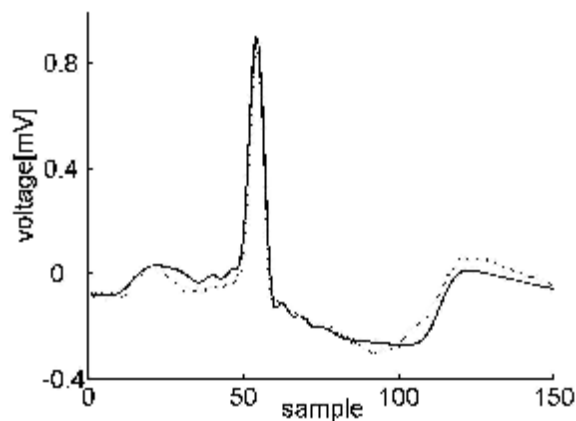


**Fig. 9** A single cycle of simulated ECG associated with WPW syndrome (dotted for the original).

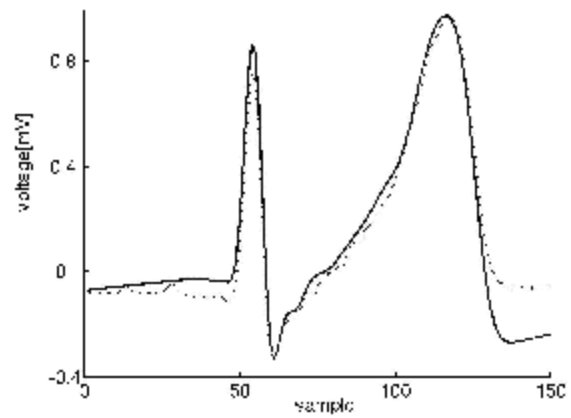


**Fig. 10** A single cycle of simulated ECG associated with hyper kalmia (dotted for the original).

Fig 12 shows the resulting HRV (RR-intervals), HR and HRV power spectrum. We can now see the required VLF, LF and HF components (as mentioned in section 2) in the HRV power spectrum of Fig. 12. Note that using the original Zeeman model does not give us any of the expected significant peaks in the power spectrum of HRV, and this means that it does not truly reflect real heart activity.

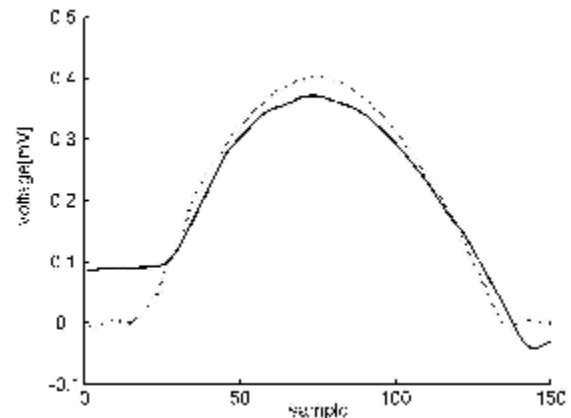


**Fig. 11** A single cycle of simulated ECG associated with ventricular flutter (dotted for the original).

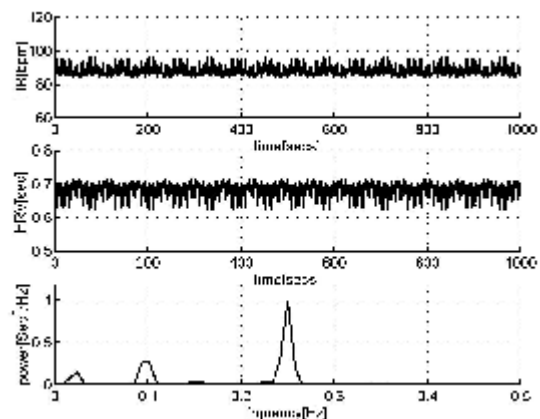


**Fig. 12** Simulated HR, HRV and normalized power spectrum of HRV (respectively) by the proposed model in (3) and (4) for a healthy subject.

We also simulated (in Fig. 13) the cases of parasympathetic blockade, high sympathetic balance and high parasympathetic balances – corresponding to autonomic regulatory sickness by changing the coupling factors  $c1-c4$  in (6).

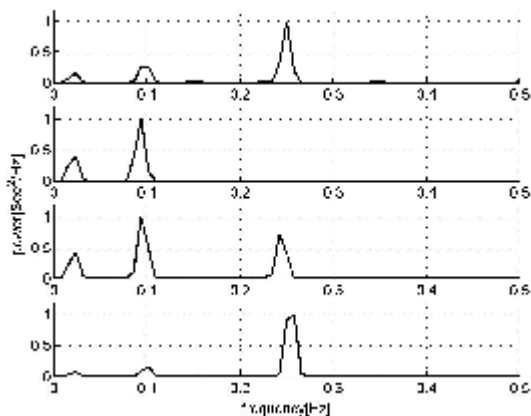


**Fig. 13** Normalized power spectrum of simulated HRV for a healthy case and three different sicknesses (see Table 1), as generated by the proposed model in (3) and (4). Top to bottom: healthy, parasympathetic blockade, high sympathetic balance and high parasympathetic balance.

## 5 Conclusion

We have proposed a new neural network approach to modeling ECG signals, and have presented simulations and measured the error performance. The advantage of this method over existing approaches, is its ability to dynamically model a much wider class of abnormal ECG's, with a low simulation error.

We have incorporated a mathematical technique to generate the RR intervals, and thus provided a more comprehensive simulation of realistic ECG's that are observed in practice. Based on the original Zeeman model (Zeeman, 1972), we have proposed a new model to generate a heart-rate time-series. The sympathetic and parasympathetic activities, give VLF, LF and HF components in the HRV power spectrum. We showed that our new model did produce these important spectral components in the simulated HRV. This means that our proposed model behaves more like the real heart, than the original Zeeman model.

In addition to modeling the abnormalities associated with the shape of ECG, we showed that our HRV model also has the capability of accurately simulating important sicknesses associated with the autonomic regularity of heart-rate.

## 6 References

- [1] McSharry PE, Clifford G, Tarassenko L, Smith LA. A dynamical model for generating synthetic electrocardiogram signals. *IEEE Transaction On biomedical Engineering*, 2003;50(3):289-294.
- [2] Malik M and Camm AJ. *Heart Rate Variability*. Futura Publication Comp., New York 1995.
- [3] Brennan M, Palaniswami M, Kamen PW. A new cardiac nervous system model for Heart rate

variability analysis. *Proc. Of the 20th Annual International Conference of IEEE Engineering in Medicine and Biology Society*, 1998;20:340-352.

- [4] McSharry PE, Clifford G, Tarassenko L, Smith LA. Method for generating an artificial RR tachogram of a typical healthy human over 24-hours. *Computer in Cardiology*, 2002;29:225-228.
- [5] Zeeman EC. *Differential equations for the heartbeat and nerve impulse*. Mathematics Institute, University of Warwick, Coventry, UK, 1972.
- [6] Tu Pierre NV. *Dynamical systems - an introduction with applications in economics and biology*, Second Edition, Springer-Verlag, 1994.
- [7] M. Y. Uctug, I. Eskandarzadeh, H, Ince, "Modelling and output power optimization of a wind turbine driven double output induction generator," *IEE Proc-Electr. Power Appl.*, Vol.141, No.2, March 1994, pp. 33-38.
- [8] Jafarnia Dabanloo N, McLernon DC, Ayatollahi A, Johari Majd V. A nonlinear model using neural networks for generating electrocardiogram signals. *IEE MEDSIP Conference Proceeding*, 2004; 41-45.
- [9] Park J and Sandberg JW. Universal approximation using radial basis functions network. *Neural Computation*, 1991; 3: 246-257.